J Nanostruct 16(4): 5264-5273, Autumn 2026

RESEARCH PAPER

Phytosynthesized of Ag@AgCl Nanocomposit; Antimicrobial, Antibiofilm Activities Against E.coli Pathogenic Isolated from Urinary Tract Infection

Masoumeh Mohammadizadeh, Fereshteh Jookar Kashi *

Department of Cell and Molecular Biology, Faculty of Chemistry, University of Kashan, Kashan 8731751167, Islamic Republic of Iran

ARTICLE INFO

Article History:
Received 26 May 2026
Accepted 29 August 2026
Published 01 October 2026

Keywords:
Ag@AgCl nanocomposites
Antimicrobials
Biofilms
Cytotoxicity
E. coli

ABSTRACT

The most common cause of urinary tract infections (UTI) is uropathogenic *Escherichia coli*, often resistant to antibiotics. *E. coli* can form biofilms on urinary catheters. The biofilm protects *E. coli* against various factors. In this study, Ag@AgCl nanocomposites were synthesized using *Trifolium pratense* L. extract as a reducing agent. The AgNPs were characterized by visible UV spectroscopy, a diffraction pattern (XRD), transmission electron microscopy (SEM), and energy dispersion spectroscopy (EDX). The AgNPs had a spherical shape with an average particle of 19 nm. Biological properties were also evaluated using biofilm inhibition, anticancer, and antimicrobial activity. The brine shrimp lethality assay was applied to assess the anticancer activity of the nanoparticles. The Ag@AgCl nanocomposites with LC_{50} (1.3 µg/ml) had the highest cytotoxicity activity. The antimicrobial activity of nanoparticles was evaluated by the agar diffusion method, minimum inhibitory concentration, and minimum bactericidal concentration in the range of 1.00 to 0.0312 and 2.00 to 0.0312, respectively. The nanocomposites exhibited a high antimicrobial effect against human *E.coli* pathogenic strains isolated from Urinary Tract Infections. The impact of biofilm inhibition on antibiotic-resistant clinical strains by silver nanoparticles showed that Ag@AgCl nanocomposites inhibited biofilm between 21.12 -97.10%.

How to cite this article
Mohammadizadeh M., Jookar Kashi F. Phytosynthesized of Ag@AgCl Nanocomposit; Antimicrobial, Antibiofilm Activities Against E.coli Pathogenic Isolated from Urinary Tract Infection. J Nanostruct, 2026; 16(4):5264-5273. DOI:10.22052/JNS.2026.04.063

INTRODUCTION

Nanotechnology describes nanoscale materials [1]. Nanotechnology is now widely innovated in scientific fields such as new therapies, medicine, tissue engineering, diagnostic concepts, drug delivery, and gene silencing [2].

The catalytic, electronic, magnetic, optical, and antimicrobial properties lead to their used in various fields, including chemistry, energy, and medicine [3].

The properties of nanoparticles depend on their size, morphology, and distribution. Nanoparticles such as silver, gold, zinc oxide, and platinum have medical and pharmaceutical applications. These nanoparticles can also be used in products such as toothpaste and cosmetics [4].

Physical and chemical methods synthesize and stabilize nanoparticles [5]. These methods include

* *Corresponding Author Email: jookar@kashanu.ac.ir*

solution reduction, photochemical reactions in reverse micelles, electrochemical reduction, heat evaporation, and radiation-assisting techniques. Physical and chemical methods have generally been applied successfully in synthesizing nanomaterials in large quantities over a short period [6].

However, these methods successfully produce nanoparticles; they harm human health and the environment due to hazardous and toxic chemicals [7]. An environmentally friendly and cost-effective method is used to produce nanoparticles [8]. The antimicrobial activity of silver nanoparticles is confirmed against a wide range of microorganisms. Also, recent studies showed that silver nanoparticles are antimicrobial agents. However, Sondi et al. reported the antibacterial effect of silver nanoparticles against *Escherichia coli as a* microbial model [9].

Generally, *E.coli, Pseudomonas aeruginosa, Enterococcus, Proteus mirabilis,* and *Klebsiella pneumonia* contribute to urinary tract infections that can form biofilms on catheters. The biofilm causes them to become resistant to antibiotics, which are a threat to health. Strategies are needed to kill the antibiotic-resistant bacteria that form a biofilm [10].

Plant compounds help synthesize nanoparticles because they do not require complex processes, including intracellular synthesis, purification, and microbial cell preservation [11].

The plants include *Solanum lycopersicums*, *Hibiscus cannabinus* stem, *Hibiscus cannabinus* leaf, *Ananas comosus,* and *Hibiscus cannabinus* leaf have been applied for green synthesis nanoparticle Ashuk Kumar et al. synthesized AgNPs using *Gloriosa superba* leaf extract [12]. The red clover (*Trifolium pratense L*.) has a high concentration of iso-flavonoids, compounds that are widely distributed in the Leguminosae family [13].

Furthermore, it has been refined in traditional medicine, which treats coughs, asthma, eczema, and eye diseases [14]. GLC-MS analysis results determined twenty-five compositions from *T. pratense* leaves, flowers, and seeds [15]. The major volatile compounds were as follows: leaves (3-hexenyl acetate, 3- hexanol, and β-okimenes), flowers (acetophenone, methyl cinnamate, and 1-phenylethanol), and seed pods (β-okimenes, unknown) [16].

For the first time, this study was conducted to synthesize novel Ag@AgCl nanocomposites using a native plant, *T. pretense*, as a new catalyst collected from Yasuj, Kohgiluyeh, and Boyer Ahmad Province, Iran. Also, the biological activity of this novel nanobiotic was performed using anticancer, antibiofilm, and antimicrobial activity against uropathogenic *Escherichia coli* isolated from urinary tract infections. Furthermore, the nanocomposites were characterized by UV-visible, XRD, FE-SEM, and EDX methods.

MATERIALS AND METHODS

Collection, identification, and extraction

Trifolium pratense flowers were collected in spring near Yasuj, Kohgiluyeh, and BoyerAhmad Province, Iran. The flowers are thoroughly washed with two liters of distilled water, stored at room temperature for two days, and then split into small pieces. To prepare the aqueous extract, 10 g *T. pratense* was placed in 100 ml sterile distilled water (ratio: 1:10) for 20 min at 50 °C. The extract was isolated with Whitman filter paper and kept for further processing at 4 °C.

Characteristics of silver nanoparticles

The plant extract was added to 1mM of $AgNO_3$ solution and incubated at 60 °C. Also, the $AgNO_3$ solution was incubated as a control. The synthesis of silver nanoparticles was confirmed using colour change to brown. To evaluate the synthesis of Ag nanoparticles, the absorbance was measured using a Schimadzu (Model No. UV 1800) spectrophotometer in the range of 300 to 800 nm at different times.

Moreover, the Fourier-transform infrared spectroscopy (FT-IR) spectra of silver nanoparticles were measured using FTIR spectrometer (Brucker, Germany) with a KBr bullet in the 4000-400 cm^1 range. The crystalline silver nanoparticles were determined by X-ray diffraction (XRD) (Panalytical, Netherlands). Furthermore, the size of the nanoparticles was evaluated by the Debye-Scherrer formula [17]. Also, the energy dispersive X-ray (EDX) and scanning electron microscope (SEM) (Tescan, Czech) were performed to investigate the morphology and the chemical composition of the nanocomposites.

Antibacterial activity

The antimicrobial effect of the nanocomposites was measured according to the protocol of the Clinical and Laboratory Standard Institute [18]. The

antibacterial effect of Ag@AgCl nanocomposites was determined against positive and negative bacteria by the agar diffusion method.

In this study, some human pathogens include *p. aeruginosa* (ATCC27853), *K. pneumonia* (ATCC 10031), *Salmonella paratyphi-A* serotype (ATCC 5702), *Staphylococcus aureus* (ATCC 29737), *Shigella dysenteriae* (PTCC 1188), *Staphylococcus epidermis* (ATCC12228), *Bacillus subtilis* (ATCC 6633), and *Escherichia coli* (ATCC 12228) were evaluated. The suspension adjusted 0.5 McFarland standard was prepared in nutrient broth at 37 °C. A 100 µl of the suspension was inoculated on Muller-Hinton agar.

Afterward, 10 µl of the nanocomposites solution (30 mg/ml) was inserted into the well. The plates were incubated at 37 °C for 24 h. The antibacterial activity was evaluated by measuring the diameter of inhibition zones.

Determination of minimum inhibition concentration

This method calculated the minimum inhibition concentration (MIC) for the susceptible microorganisms to the nanocomposites. The MIC value was evaluated using the microdilution method. For this purpose, 95 µl of TSB medium, 5µl bacterial suspension adjusted 0.5 McFarland, and 100 µl of different concentrations of silver nanoparticles (0.03125, 0.0625, 0.025, 0.25, 0.5). (0, 1 and 2 mg/ml) were added to each well. Furthermore, 195 µl of culture medium and 5 µl of the suspension were used as controls. The microplate was then incubated at 37 °C for 24 h. Microbial growth was characterized by turbidity at the bottom of the well.

To measure lethality, after 24 h, 5µl of each clean well was inoculated on a nutrient agar medium and incubated at 37 °C for 24 h. The concentration that did not grow after 24 h killed the bacteria, and the lowest concentration was considered the minimum bactericidal concentration.

Biofilm inhibition assay

Sixteen human pathogenic *E.coli* strains were isolated and collected from suspected infected Urinary tract infection (UTI) patients. According to microplate biofilm assay, the antibiofilm effect of Ag@AgCl nanocomposites was evaluated against *E.coli* strains.

At first, 100 µl of the nanoparticles (2mg/ml) and 100 µl of each diluted strain were added to each well. Moreover, 200 µl of TSB and the bacteria suspensions were negative and positive control, respectively. The microplate was incubated for 24 h at 37 °C. The 1% crystal violet was then added to each well, and after 10 min, the crystal violet was washed with distilled water and allowed to dry. Finally, 200 µl of acetic acid was added to each well, and after 15 min, the optical density (OD) was measured using ELISA at 570 nm. The following formula calculated the percentage of biofilm inhibition in the samples [19].

Inhibition Percentage = 100× (C-B) - (T-B)

In this equation, C equals the mean biofilm absorbance, the mean absorbance of the well containing the sample affected. B is the mean absorbance of the wells containing the medium (control). It was also repeated three times to ensure the test.

Evaluation of anticancer activity

The cytotoxicity activity of biosynthesized Ag@AgCl nanocomposites was investigated using Brine Shrimp Lethality Assay (BSLA).

Artemia salina eggs were grown in artificial seawater (pH 9) for 48 h. The different concentrations (0, 10, 100, 300, 500, 700, and 1000 µg) of biosynthesized Ag NPs were added to the vial, including 5 ml seawater and ten brine shrimp larvae, and incubated at 25 °C for 24h. Brine shrimp death was observed at regular intervals. Vincristine sulfate (VS) was applied as a positive control. These tests were repeated three times. The lethality percentage was recorded according to formula [20].

Lethality percentage = [(m-M)/s] ×100

m: Average number of dead larvae sampled, M: Average number of dead larvae control, s: Average number of live larvae control.

RESULTS AND DISCUSSION

Characterization of nanoparticles

The formation of extracellular was observed with a change in color from yellowish to deep brown due to the excitation of the localized surface plasmon vibrations of the nanoparticles.

The changing color from yellowish to brown confirmed the synthesis of the nanoparticles.

One of the properties of metal nanoparticles

is their optical properties, which change [21]. The color change indicated the biosynthesis of silver nanoparticles using an aqueous extract of *T. pretense* (Fig. 1).

Free electrons in silver nanoparticles are excited by visible light absorption and transmitted

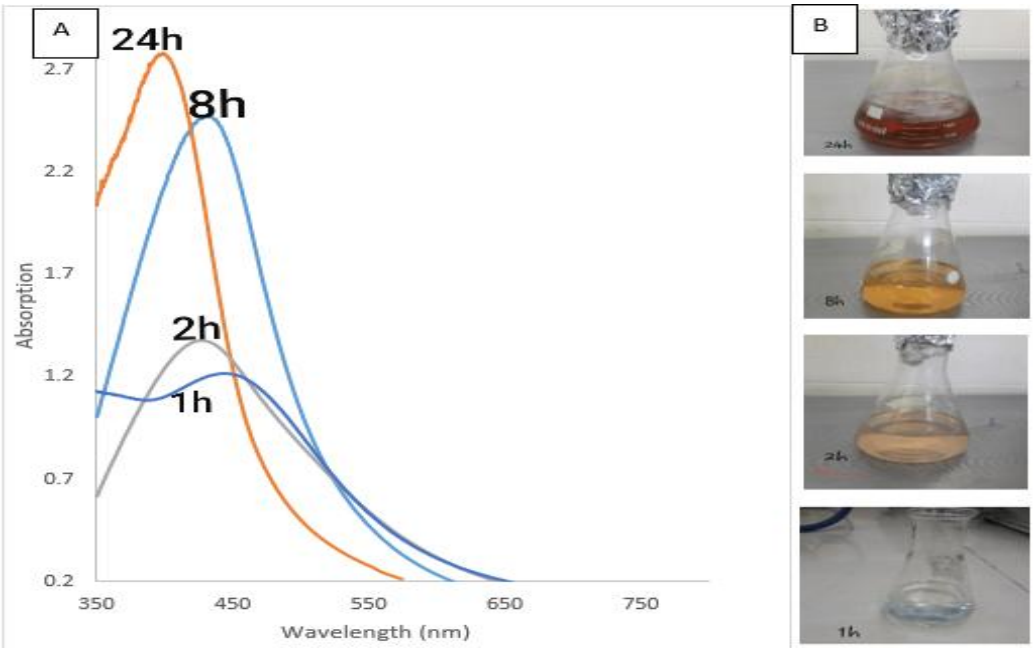

Fig. 1. Spectrophotometric analysis (A) and visible observation (B) of biosynthesis of $AgNp_s$ over time.

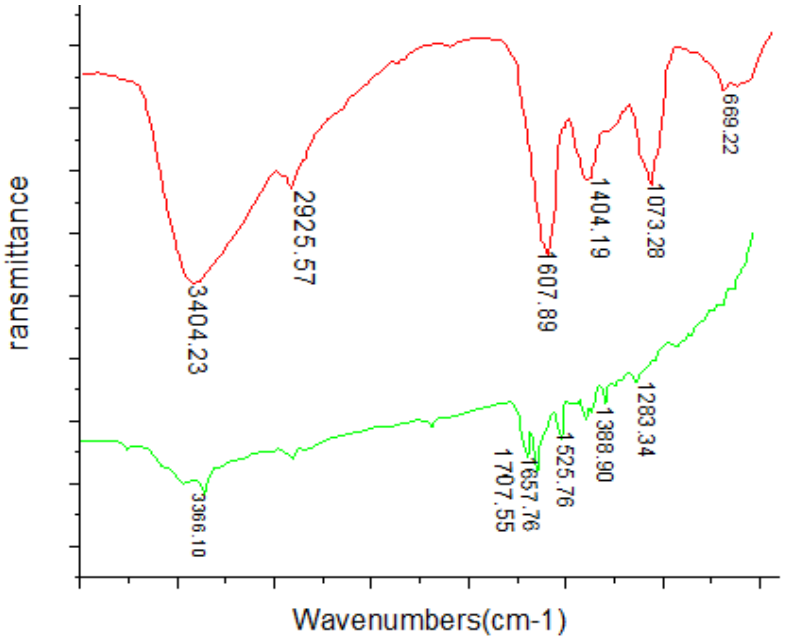

Fig. 2. FT-IR spectra of the extract (B) and the silver nanoparticles synthesized from the extract (E).

to higher energy levels. The unstable electrons return to their original energy levels and emit a photon simultaneously [22].

Fig. 1 shows a maximum wavelength of about (450 nm), similar to other researchers [23]. The optimal conditions for preparing these nanoparticles were 1mM of silver nitrate and 5 ml of aqueous extract at 65 °C for 24 h. The effect of contact time (0, 2, 8, 12, 24h) on the formation of nanoparticles was investigated under constant conditions.

As exhibited in Fig. 1, with the increased time, an increasing trend in absorbance was exhibited.

FTIR

Comparing the spectral pattern of silver nanoparticles and the extract showed that nanoparticles contain compounds in the extract. They are usually formed as a layer around the nanoparticles and can play a role in the stability of nanoparticles. The results showed peaks in regions 3404 cm^{-1} determined the OH bond in phenols and alcohols. Moreover, the absorption band indicated in region 2925 cm^{-1} corresponds to CH stretching vibration in alkyls (methylene group), and 1607 cm^{-1} corresponds to NH bonds in first amines (Fig. 2). Furthermore, the band at 1404 cm^{-1} corresponding OH stretching indicates that phenols. The absorption band determined in region 1073 cm^{-1} corresponds to the CO stretching in the first alcohols. Phenolic compounds present in the plant are among the major contributors to reducing silver ions and the synthesis of nanoparticles.

SEM analysis

The surface morphology and structure of the synthesized silver nanoparticles were characterized using SEM. Fig. 3 exhibited that the silver nanoparticle was almost spherical, ranging between 19 and 46 nm and having an average size of 34.42 nm. The results of the size distribution analysis of silver nanoparticles are shown in (Fig. 3).

EDX

The EDX result confirmed the presence of silver as a major element. Moreover, the present O,

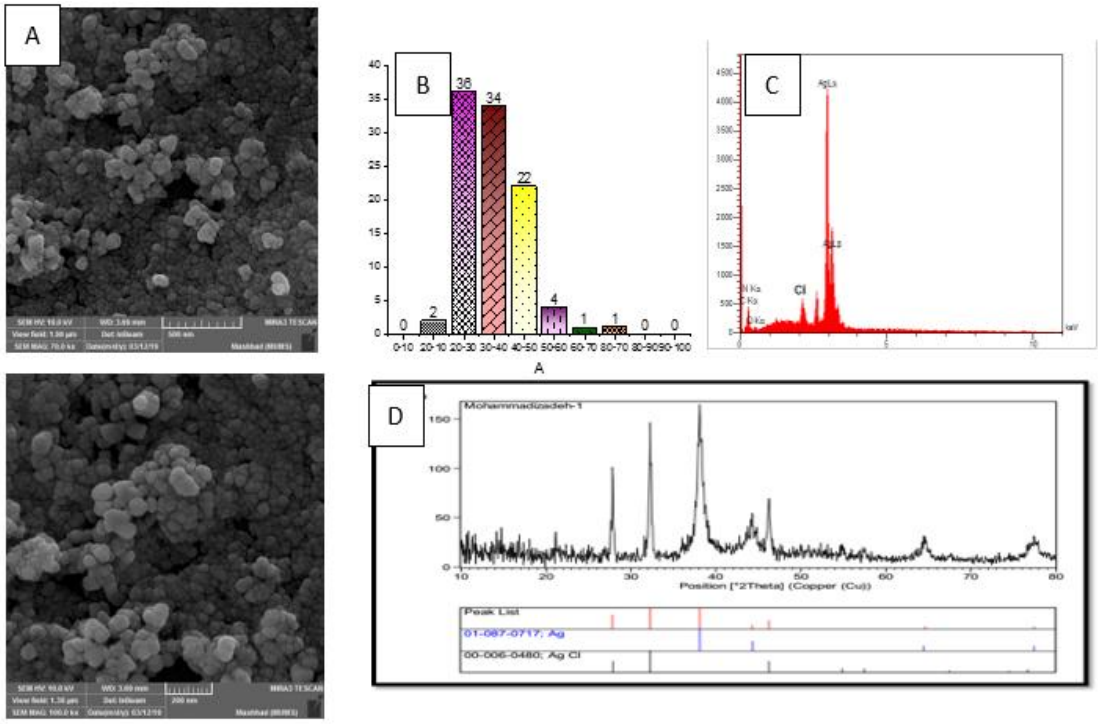

Fig. 3. SEM images of the silver nanoparticles synthesized from the extract (A). Frequency distribution of the size of silver nanoparticles synthesized from the extract (B). X-ray diffraction energy spectra for the silver nanoparticles synthesized from the extract (C). XRD spectra of the silver nanoparticles synthesized from the extract (D).

C, and N were determined in the EDX spectrum (Fig. 3). The presence of biomaterial is one of the advantages of nanoparticles synthesized using plant extracts compared to chemical methods.

Similar results also reported the formation of silver nanoparticles performed using *Artemisia nilagirica* leaf and *Artocarpus heterophyllus* seed extract [24].

XRD

X-ray diffraction is used to study the structure of crystalline materials. The spectral region results can obtain information on the structure, material, and quantities of the elements [25]. X-ray diffraction analysis was used to investigate and study the synthesized silver nanoparticles (Fig. 3).

The average crystal size was calculated by calculating the width of peaks formed in the samples using the Debay-Scherer formula [26].

$$D= (0.9\lambda/\beta \cos\Theta)$$

Where β is the width of the peaks at half the maximum height, λ is the X-ray wavelength equal to 54.1 nm. Moreover, Θ is the angle between the reflected beam and the radiation, and D is the crystal size. As shown in the figure, clear peaks in the areas 2Θ = 27.82, 32.25, 38.07, 44.25, 46.25, 64, 57, and 77.3 are the reason for the successful synthesis of nanoparticles. The presence of sharp peaks in the patterns indicates a high degree of crystallinity for the nanoparticles. The average size of the synthesized crystal was estimated at 22.25 nm, utterly consistent with SEM results.

Antimicrobial activity

The antimicrobial effect of the silver nanoparticles, the extract, and the composite of extract and silver nanoparticles were measured by the present or absent zone of the inhibition, and the results are shown in Table1.

Yazdani et al. reported that silver quantum dots synthesized by *Teucrium polium* L. had antimicrobial activity [27].

Silver nanoparticles synthesized by *Eugenia roxburghii* DC. were evaluated against bacterial biofilms. Their results showed that the silver nanoparticles inhibited biofilms [28].

The results showed that the nanoparticles had an antimicrobial effect. In contrast, the extract shows no antimicrobial activity.

The nanoparticles showed a zone of inhibition against *B. subtilis, S. epidermidis,* and *P. aeruginosa* (9 mm). Moreover, *S.paratyphi A serotype* exhibited the inhibition zone (10 mm), and the zone of *S. aureus* was 7 mm. The composite of extract and silver nanoparticles has no antimicrobial effect except for two strains: *B. subtilis* (9 mm) and *S. epidermidis* (7 mm).

Allafchian et al. reported the antibacterial effect of silver nanoparticles against Gram-positive (*S. aureus* and *B. cereus*) and Gram-negative (*S. typhimurium* and *E.coli*) bacteria using the agar well diffusion. These nanoparticles were synthesized by *Phlomis cancellata* Bunge leaf extract. Their results proved to be almost parallel with our findings [6].

Furthermore, in the study by Hashoosh et al., silver nanoparticles synthesized by Aloe vera plant and Aloe vera extract had different antibacterial effects against Gram-negative bacteria (*E.coli*) and Gram-positive bacteria (*S.aureus*). The results showed that the aqueous extract of Aloe vera had no inhibitory effect. In contrast, silver nanoparticles

Table 1. Antimicrobial activity of silver nanoparticles and the plant extract.

Bacterial strains	Silver nanoparticles	Composite nanoparticles	Extracts
	Inhibition zones (mm)		
B. subtilis	9	9	-
S. epidermidis	9	7	-
S. aureus	7	-	-
E. coli	-	-	-
K. pneumonia	-	-	-
S. paratyphi A serotype	10	-	-
P. aeruginosa	10	-	-
S.dysenteriae	-	-	-
C. albicans	-	-	-

A dash (-) determine no antimicrobial effect.

had an inhibitory effect against *E.coli* and *S.aureus* [4]. According to a recent study, Ag/AgCl nanoparticles synthesized from *Staphylococcus pasteuri* ZAR1 exhibited antibacterial effect on 66 pathogenic strains [29].

Nazar Ul Islam et al. reported synthesized silver nanoparticles using *Prunus armeniaca*. They investigated the antimicrobial properties of the nanoparticles and the extract against *S. aureus*, *E.coli*, and *P. aeruginosa* with the diameter of inhibition zones 18, 10.2, and 11.2 mm, respectively. However, the plant extract alone did not have antimicrobial activity [30]. In another study by S. Yallappa et al., copper nanoparticles synthesized using an aqueous extract of *Terminalia arjuna* tree bark showed good antimicrobial activity against S. *aureus*, *E.coli*, *S. typhi,* and *P. aeruginosa* [31].

Biofilm Inhibition

The antibacterial effect of the silver nanoparticles was evaluated against sixteen *E.coli*

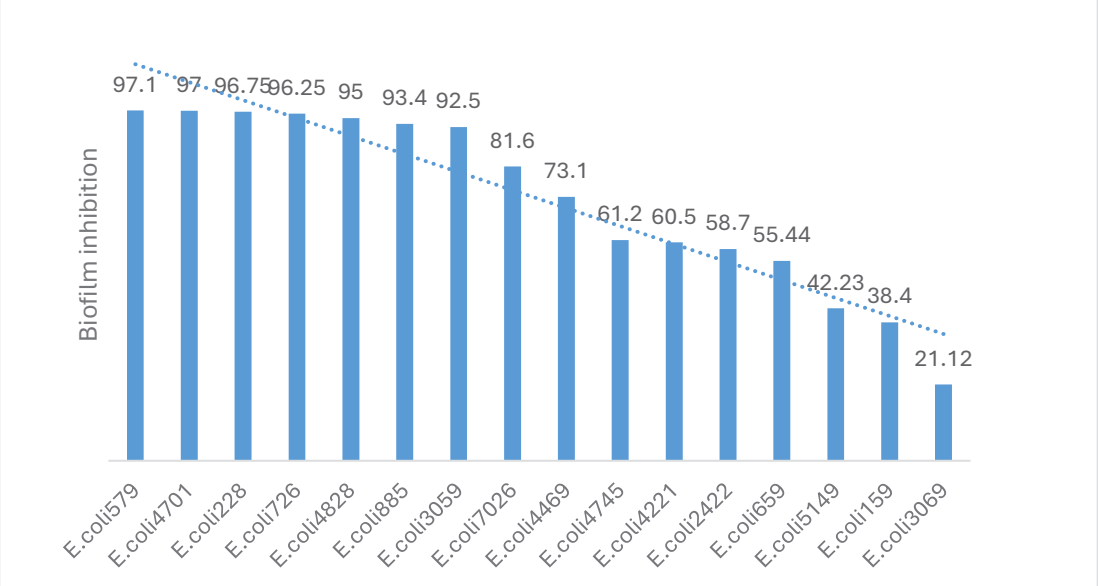

Fig. 4. Biofilm inhibition percentage of the silver nanoparticles against *E.coli* clinical strains.

Table 2. Results of MIC and MBC (mg /ml), and biofilm formation ability.

No.	Bacteria	Code	MIC mg /ml	MBC mg /ml	Biofilm formation power	Biofilm inhibition%	No.	Bacteria	Code	MIC mg /ml	MBC mg /ml	Biofilm formation power	Biofilm inhibition%
1	*E. coli*	4221	0.25	0.50	Medium	60.5	9	*E. coli*	726	0.031	0.062	Strong	96.25
2	*E. coli*					92.5	10	*E. coli*		2	5	Strong	96.7
3	*E. coli*	3059	0.062	0.25	Strong	81.6	11	*E. coli*	228	0.031	0.031	Strong	97.1
4	*E. coli*		5	0.062	Strong	38.4	12	*E. coli*		2	2	Weak	42.23
5	*E. coli*	7026	0.062	5	Weak	97	13	*E. coli*	579	0.031	0.062		
6	*E. coli*		5	1.00		73.1	14	*E. coli*		2	5	Strong	93.4
7	*E. coli*	159	0.50		Strong	58.7	15	*E. coli*	5149	0.50	0.50		
8	*E. coli*			0.031	Medium	61.2	16	*E. coli*				Weak	21.12
		4701	0.031	2	Medium				885	0.031	0.031	Medium	55.44
			2	0.25						2	2	Strong	95
		4469	0.25	1.00	Medium				3069				
			0.25							1.00	2.00		
		2422		0.25					659	0.25	0.25		
			0.25							0.062	0.25		
		4745							4828	5			

strains isolated from patients with urinary tract infections. The results show that the MIC and MBC of silver nanoparticles range from 1.00 to 0.0312 and 2.00 to 0.0312, respectively (Table 2).

The biofilm formation ability was measured for each assay as a control. The percentage of biofilm inhibition of the silver nanoparticles was between 21.12-97.10%. The nanoparticles exhibited high ability antibiofilm against *E. coli* 579*, E. coli* 4701*, E. coli* 228*, E. coli* 726*, E. coli* 4828*, E. coli* 885, and *E. coli* 3059*.* Furthermore, the lowest ability antibiofilm was against *E. coli* 5149*.*

Biofilm inhibitory activity of nanoparticles synthesized from *Cordia. Dichotoma* was evaluated. The results showed that silver nanoparticles (100 µg/ml) inhibited *S.aureus* and *E.coli* biofilm *(*92% and 95%) after 12h [32].

Morones-Amirez et al. reported that AgNPs inhibited biofilm activity by approximately 20% [33].

The other report evaluated the antibiofilm effect of biosynthesized Ag/AgCl composite against pathogenic bacterial strains. Their results showed that the composite inhibited biofilm in the 5-100% range [34].

Cytotoxicity

The anticancer activity of the silver nanoparticles and the percentage of dead larvae were determined at different concentrations (µg/ml).

The previous study determined that LC_{50} (0.5-1 mg/ml) was weak in the toxicity against *A. salina.* Moreover, The LC_{50} between 0 and 0.1 mg/ml exhibited high toxicity and 0.1-0.5 mg/ml moderate cytotoxicity. LC_{50} above 1 mg/ml indicated a lack of toxicity against *A. salina* [35].

Our study showed that the silver nanoparticles

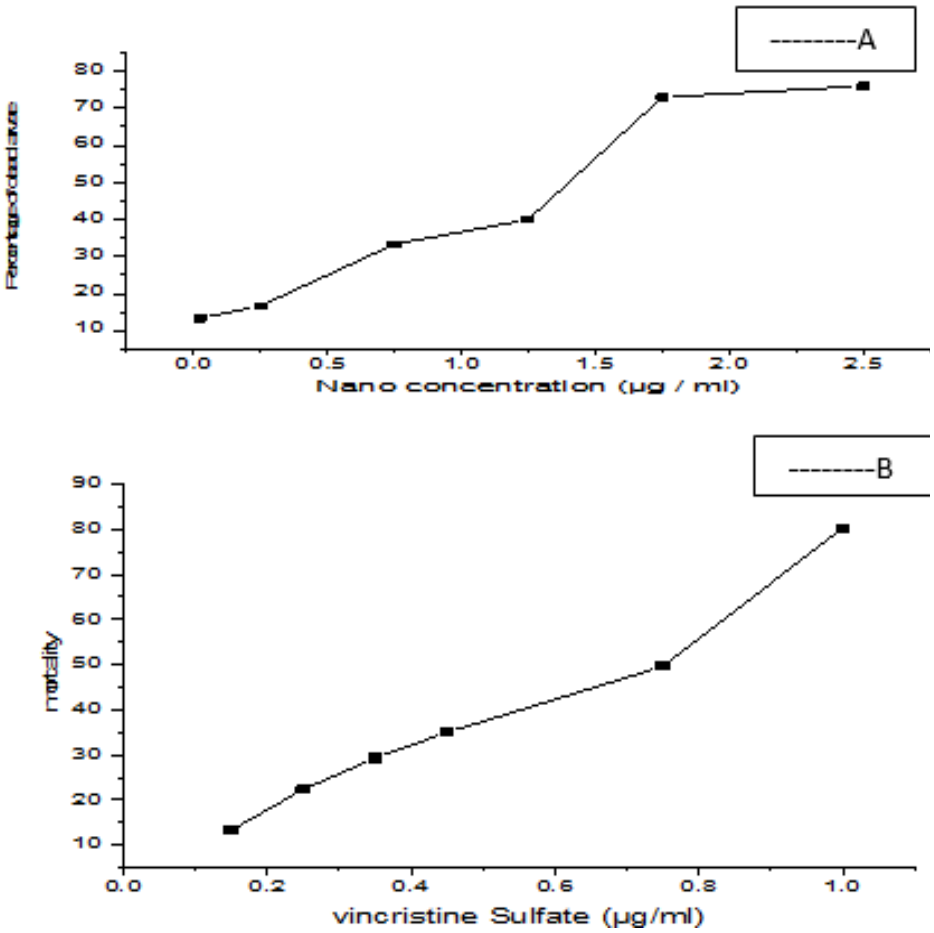

Fig. 5. Cytotoxicity effect at different concentrations of the silver nanoparticles (A) and vincristine sulfate (B).

with LC_{50} 1.3 µg/ml had high cytotoxicity and anticancer properties. Furthermore, the LC_{50} of vincristine sulfate was 0.751 µg/ml as a positive control. Based on these results, *T. pratense* L. extract showed high cytotoxicity (Fig. 5).

A similar research reported copper nanoparticles synthesized by *Prunus mahaleb* L. have cytotoxic and anticancer effects, according to the results of BSLA [36].

CONCLUSION

For the first time in the present study, silver nanoparticles were synthesized using the *T. pratense*. The antimicrobial and antibiofilm activity of the nanoparticles was determined. Additionally, the formation of silver nanoparticles was confirmed using UV-Vis, XRD, SEM, EDX, and FTIR. However, this study reports a novel, rapid, economical, and environmentally friendly procedure for producing silver nanoparticles.

Based on the results, the nanoparticles have anticancer, antimicrobial, and antibiofilm activity against UTI. Silver nanoparticles may play a role in neutralizing cell adhesives, thus preventing biofilm formation. Bacterial biofilm is highly resistant to antibiotics. Therefore, silver nanoparticles may play a major role in biofilm formation on urinary catheters.

ACKNOWLEDGEMENT

We are grateful to University of Kashan for supporting this work.

CONFLICT OF INTEREST

The authors declare that there is no conflict of interests regarding the publication of this manuscript.

REFERENCES

1. Saxena A, Tripathi RM, Zafar F, Singh P. Green synthesis of silver nanoparticles using aqueous solution of Ficus benghalensis leaf extract and characterization of their antibacterial activity. Mater Lett. 2012;67(1):91-94.
2. In vitro antioxidant, antimicrobial and cytotoxic activities and green biosynthesis of silver and gold nanoparticles using Callistemon citrinus leaf extract. Journal of Applied Pharmaceutical Science. 2017.
3. Anandalakshmi K, Venugobal J, Ramasamy V. Characterization of silver nanoparticles by green synthesis method using Pedalium murex leaf extract and their antibacterial activity. Applied Nanoscience. 2015;6(3):399-408.
4. hashoosh SI, Fadhil AMA, Al-Ani Nk. Production of Ag nanoparticles Using Aloe vera Extract and its Antimicrobial Activity. Journal of Al-Nahrain University Science. 2014;17(2):165-171.
5. Sharma VK, Yngard RA, Lin Y. Silver nanoparticles: Green synthesis and their antimicrobial activities. Advances in Colloid and Interface Science. 2009;145(1-2):83-96.
6. Allafchian AR, Mirahmadi-Zare SZ, Jalali SAH, Hashemi SS, Vahabi MR. Green synthesis of silver nanoparticles using phlomis leaf extract and investigation of their antibacterial activity. Journal of Nanostructure in Chemistry. 2016;6(2):129-135.
7. Dhand V, Soumya L, Bharadwaj S, Chakra S, Bhatt D, Sreedhar B. Green synthesis of silver nanoparticles using Coffea arabica seed extract and its antibacterial activity. Materials Science and Engineering: C. 2016;58:36-43.
8. Behravan M, Hossein Panahi A, Naghizadeh A, Ziaee M, Mahdavi R, Mirzapour A. Facile green synthesis of silver nanoparticles using Berberis vulgaris leaf and root aqueous extract and its antibacterial activity. Int J Biol Macromol. 2019;124:148-154.
9. Krishnaraj C, Jagan EG, Rajasekar S, Selvakumar P, Kalaichelvan PT, Mohan N. Synthesis of silver nanoparticles using Acalypha indica leaf extracts and its antibacterial activity against water borne pathogens. Colloids Surf B Biointerfaces. 2010;76(1):50-56.
10. Lopez-Carrizales M, Velasco KI, Castillo C, Flores A, Magaña M, Martinez-Castanon GA, et al. In Vitro Synergism of Silver Nanoparticles with Antibiotics as an Alternative Treatment in Multiresistant Uropathogens. Antibiotics. 2018;7(2):50.
11. Ravichandran V, Vasanthi S, Shalini S, Ali Shah SA, Harish R. Green synthesis of silver nanoparticles using Atrocarpus altilis leaf extract and the study of their antimicrobial and antioxidant activity. Mater Lett. 2016;180:264-267.
12. Annamalai A, Christina VLP, Sudha D, Kalpana M, Lakshmi PTV. Green synthesis, characterization and antimicrobial activity of Au NPs using Euphorbia hirta L. leaf extract. Colloids Surf B Biointerfaces. 2013;108:60-65.
13. Dixon RA. PHYTOESTROGENS. Annu Rev Plant Biol. 2004;55(1):225-261.
14. Booth NL, Overk CR, Yao P, Totura S, Deng Y, Hedayat AS, et al. Seasonal Variation of Red Clover (Trifolium pratense L., Fabaceae) Isoflavones and Estrogenic Activity. Journal of Agricultural and Food Chemistry. 2006;54(4):1277-1282.
15. Buttery RG, Kamm JA, Ling LC. Volatile components of red clover leaves, flowers, and seed pods: possible insect attractants. Journal of Agricultural and Food Chemistry. 1984;32(2):254-256.
16. Figueiredo R, Rodrigues A, Doceucosta M. Volatile composition of red clover (Trifolium pratense L.) forages in Portugal: The influence of ripening stage and ensilage. Food Chem. 2007;104(4):1445-1453.
17. Ajitha B, Ashok Kumar Reddy Y, Reddy PS. Biogenic nano-scale silver particles by Tephrosia purpurea leaf extract and their inborn antimicrobial activity. Spectrochimica Acta Part A: Molecular and Biomolecular Spectroscopy. 2014;121:164-172.
18. An Overview of the Clinical and Laboratory Standards Institute (CLSI) and Its Impact on Antimicrobial Susceptibility Tests. Antimicrobial Susceptibility Testing Protocols: CRC Press; 2007. p. 15-20. http://dx.doi.org/10.1201/9781420014495-6
19. Stepanović S, Vuković D, Hola V, Bonaventura GD, Djukić S, Ćirković I, et al. Quantification of biofilm in microtiter plates: overview of testing conditions and practical recommendations for assessment of biofilm production by staphylococci. APMIS. 2007;115(8):891-899.
20. Arulvasu C, Jennifer SM, Prabhu D, Chandhirasekar D. Toxicity Effect of Silver Nanoparticles in Brine Shrimp

nArtemia. The Scientific World Journal. 2014;2014:1-10.
21. Mohamed MB, Volkov V, Link S, El-Sayed MA. The `lightning' gold nanorods: fluorescence enhancement of over a million compared to the gold metal. Chem Phys Lett. 2000;317(6):517-523.
22. Thangaraju N, Venkatalakshmi RP, Chinnasamy A, Kannaiyan P. Synthesis of Silver Nanoparticles and the Antibacterial and Anticancer Activities of the Crude Extract of Sargassum Polycystum C. Agardh. Nano Biomed Eng. 2012;4(2).
23. Singh PK, Bhardwaj K, Dubey P, Prabhune A. UV-assisted size sampling and antibacterial screening of Lantana camara leaf extract synthesized silver nanoparticles. RSC Adv. 2015;5(31):24513-24520.
24. Anandalakshmi K, Venugobal J. Electrochemical and antibacterial activity of silver nanoparticles synthesized using Mukia madarasapattana leaf extract. Journal of Plant Biochemistry and Biotechnology. 2020;30(2):396-399.
25. Cullity BD, Weymouth JW. Elements of X-Ray Diffraction. Am J Phys. 1957;25(6):394-395.
26. Ajitha B, Ashok Kumar Reddy Y, Sreedhara Reddy P. Biosynthesis of silver nanoparticles using Plectranthus amboinicus leaf extract and its antimicrobial activity. Spectrochimica Acta Part A: Molecular and Biomolecular Spectroscopy. 2014;128:257-262.
27. Yazdani M, Jookar Kashi F, Seyed Hosseini E. An environmentally safe approach for the facile synthesis of anti-mutagenic fluorescent quantum dots: Property investigation and the development of novel antimicrobial applications. Arabian Journal of Chemistry. 2023;16(7):104811.
28. Giri AK, Jena B, Biswal B, Pradhan AK, Arakha M, Acharya S, et al. Green synthesis and characterization of silver nanoparticles using Eugenia roxburghii DC. extract and activity against biofilm-producing bacteria. Sci Rep. 2022;12(1).
29. Fakher SN, Kashi FJ. Microbial Synthesized Ag/AgCl Nanoparticles Using Staphylococcus pasteuri sp. nov., ZAR1: Antimutagenicity, Antimicrobial Agent. Journal of Inorganic and Organometallic Polymers and Materials. 2021;31(4):1688-1703.
30. Islam NU, Amin R, Shahid M, Amin M. Gummy gold and silver nanoparticles of apricot (Prunus armeniaca) confer high stability and biological activity. Arabian Journal of Chemistry. 2019;12(8):3977-3992.
31. Khan UU, Munir S, Khan AA. Synthesis and Characterization of Copper Oxide (CuO) and Nickel Doped Copper Oxide Ni(CuO) Multifunctional Nanoparticles for Biological Applications. MDPI AG; 2025. http://dx.doi.org/10.20944/preprints202508.1420.v1
32. Bharathi D, Vasantharaj S, Bhuvaneshwari V. Green synthesis of silver nanoparticles using Cordia dichotoma fruit extract and its enhanced antibacterial, anti-biofilm and photo catalytic activity. Materials Research Express. 2018;5(5):055404.
33. Gurunathan S, Han JW, Kwon D-N, Kim J-H. Enhanced antibacterial and anti-biofilm activities of silver nanoparticles against Gram-negative and Gram-positive bacteria. Nanoscale Research Letters. 2014;9(1).
34. Kordzangeneh H, Jookar Kashi F. A new Bacillus Paralicheniformis sp. Tmas-01 as bioreactor for synthesis of Ag/AgCl composite–different effects of biological and Rodamin B dye decolorization, anticancer, genotoxic activity. Arch Microbiol. 2022;204(12).
35. Wiji Prasetyaningrum P, Bahtiar A, Hayun H. Synthesis and Cytotoxicity Evaluation of Novel Asymmetrical Mono-Carbonyl Analogs of Curcumin (AMACs) against Vero, HeLa, and MCF7 Cell Lines. Sci Pharm. 2018;86(2):25.
36. Dashtizadeh Z, Jookar Kashi F, Ashrafi M. Phytosynthesis of copper nanoparticles using Prunus mahaleb L. and its biological activity. Materials Today Communications. 2021;27:102456.